ELSEVIER

Chemistry & Biology 8 (2001) 369–378

Chemistry & Biology

www.elsevier.com/locate/chembiol

Research Paper

Possible cause of G·C → C·G transversion mutation by guanine oxidation product, imidazolone

Katsuhito Kino, Hiroshi Sugiyama*

Division of Biofuctional Molecules, Institute of Biomaterials and Bioengineering, Tokyo Medical and Dental University, 2-3-10 Surugadai, Kanda, Chiyoda, Tokyo 101-0062, Japan

Received 5 December 2000; revisions requested 6 February 2001; revisions received 22 February 2001; accepted 27 February 2001
First published online 22 March 2001

Abstract

Background: The genome is constantly assaulted by oxidation reactions which are likely to be associated with oxygen metabolism, and oxidative lesions are generated by many types of oxidants. Such genotoxin-induced alterations in the genomic message have been implicated in aging and in several pathophysiological processes, particularly those associated with cancer. The guanine base (G) in genomic DNA is highly susceptible to oxidative stress due to having the lowest oxidation potential. Therefore, G·C → T·A and G·C → C·G transversion mutations frequently occur under oxidative conditions. One typical lesion of G is 8-oxo-7,8-dihydro-guanine (8-oxoG), which can pair with A. This pairing may cause G·C → T·A transversion mutations. Although the number of G·C → C·G transversions is rather high under specific oxidation conditions such as riboflavin photosensitization, the molecular basis of G·C → C·G transversions is not known.

Results: To determine which oxidative products are responsible for G·C → C·G transversion mutations, we photooxidized 5′-d(AAAAAAGGAAAAAA)/5′-d(TTTTTTCCTTTTTT) using either riboflavin or anthraquinone (AQ) carboxylate under UV irradiation. Prolonged low-temperature (4°C) enzymatic digestion of photoirradiated sample indicated that under both conditions the amount of 8-oxo-7,8-dihydro-2′-deoxyguanosine (8-oxodG) initially increased with decreasing amounts of 2′-deoxyguanosine (dG), then decreased with the formation of 2-amino-5-[(2-deoxy-β-D-*erythro*-pentofuranosyl)amino]-4*H*-imidazol-4-one (dIz), suggesting that nascent 8-oxoG was further oxidized to 2,5-diamino-4*H*-imidazol-4-one (Iz) in duplex DNA. Photoirradiation of an AQ-linked oligomer with a complementary strand containing 8-oxoG indicated that 8-oxoG residues were oxidized to Iz. These results indicate that Iz is formed from 8-oxoG through long-range hole migration. Primer extension experiments using a template containing Iz demonstrated that only dGTP is specifically incorporated opposite Iz suggesting that specific Iz·G base pairs are formed. The 'reverse' approach consisting of DNA polymerization using dIzTP showed that dIzTP is incorporated opposite G, further confirming the formation of a Iz·G base pair.

Conclusions: HPLC product analysis demonstrated that Iz is a key oxidation product of G through 8-oxoG in DNA photosensitized with riboflavin or anthraquinone. Photoreaction of AQ-linked oligomer confirmed that Iz is formed from 8-oxoG through long-range hole migration. Two sets of primer extension experiments demonstrated that Iz can specifically pair with G in vitro. Specific Iz·G base pair formation can explain the G·C → C·G transversion mutations that appear under oxidative conditions.

Keywords: G·C → C·G transversion mutation; 2,5-Diamino-4*H*-imidazol-4-one (Iz); Iz·G base pair; Oxidation of 8-oxoG

1. Introduction

The genome, which stores all information of life, is constantly assaulted by endogenous and exogenous oxidative stress. Independent of the source, reactive species are potent genotoxins that attack DNA and generate oxidative lesions [1]. These genotoxin-induced alterations in the genomic message have been implicated in aging and in several pathophysiological processes, particularly those associated with cancer [2]. From bacteria to humans, various types of repair enzymes maintain the integrity of the genome. Many studies have demonstrated the importance of DNA repair in the prevention of diseases such as cancer. Therefore, considerable effort has focused upon understanding the mechanisms of oxidative DNA damage and

* Correspondence: Hiroshi Sugiyama;
E-mail: sugiyama@chem.i-mde.tmd.ac.jp

1074-5521/01/$ – see front matter
PII: S1074-5521(01)00019-9

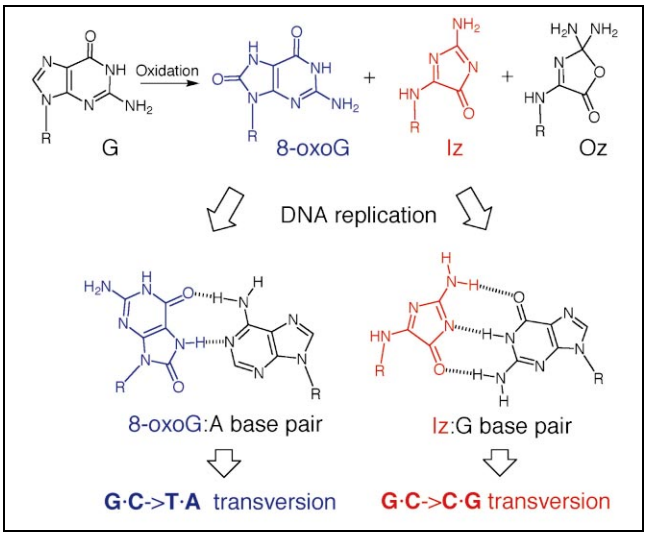

Fig. 1. Oxidative products of guanine and proposed scheme for G·C→T·A and G·C→C·G transversion mutations caused by 8-oxoG and Iz, respectively.

repair [3,4]. G is highly susceptible to oxidative stress in the genome, as it has the lowest redox potential [5]. A typical lesion is 8-oxo-7,8-dihydro-guanine (8-oxoG) (Fig. 1), which is formed under various oxidative conditions. Thus, the biological impact of 8-oxoG has been extensively investigated [4,6–12]. Since 8-oxoG can pair with A in the Hoogsteen mode (Fig. 1), 8-oxoG·A base pairs are believed to cause G·C→T·A transversion mutations [9]. Although the frequency of G·C→C·G transversions is considerably high under oxidative stress [13–27], the oxidative lesion which causes G·C→C·G transversions is unknown. Cadet et al. reported that 2-amino-5-[(2-deoxy-β-D-*erythro*-pentofuranosyl)amino]-4*H*-imidazol-4-one (dIz) (Fig. 1) and its hydrolysis product 2,2-diamino-4-[(2-deoxy-β-D-*erythro*-pentofuranosyl)amino]-5(2*H*)-oxazolone (dOz) are major oxidation products of 2′-deoxyguanosine (dG) [28,29]. We recently demonstrated that dIz is a key UV detectable product formed in double stranded DNA during the photooxidation with riboflavin and we proposed that 2,5-diamino-4*H*-imidazol-4-one (Iz) forms base pairs with G to induce G·C→C·G transversion mutation (Fig. 1) [30].

2. Results

2.1. Formation of Iz from G in photooxidized DNA with riboflavin or anthraquinone (AQ)

Iz is formed from G under various oxidative conditions such as γ-radiation, photosensitization with riboflavin and Mn-TMPyP/$KHSO_5$ [28–32]. Cadet et al. investigated the mechanism of the formation of dIz from dG was and found that Type I photosensitization mechanism is predominant for riboflavin with minor contribution of the

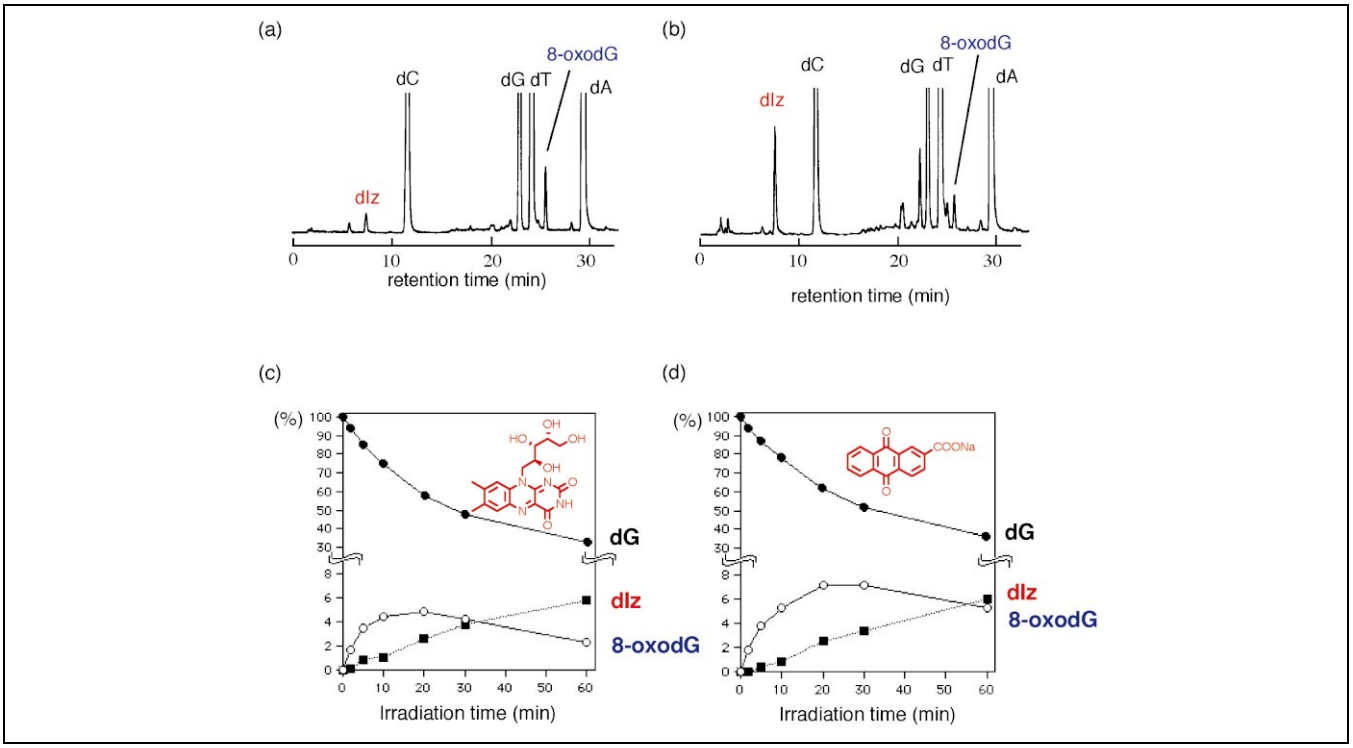

Fig. 2. HPLC analysis (254 nm) of photooxidation of 5′-AAAAAAGGAAAAAA-3′/5′-TTTTTTCCTTTTTT-3′ with photosensitizer, riboflavin after (a) 10 and (b) 60 min photoirradiation. Quantitative analysis of the enzymatic digestion of reaction mixture with (c) riboflavin or (d) AQ. Oxidized oligomer was digested with nuclease P1 and alkaline phosphatase. The amount of deoxyguanosine (black circles), 8-oxoG (open circles) and Iz (black squares) are shown after incubation periods of 0, 2, 5, 10, 20 30 and 60 min.

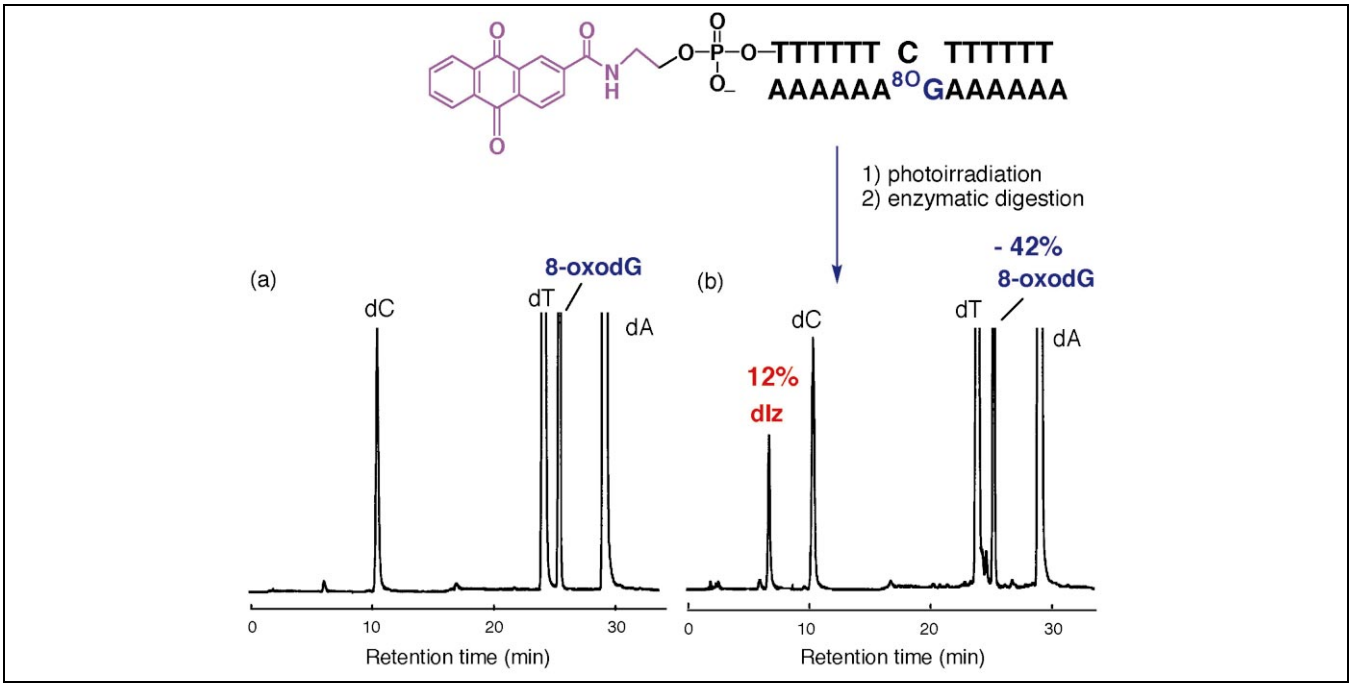

Fig. 3. Photooxidation of AQ-linked oligomer, 5′-AQ-d(TTTTTTCTTTTTT), with complementary strand, 5′-d(AAAAAA^{8O}GAAAAAA). HPLC analysis (254 nm) of enzymatic digestion mixture after (a) no and (b) 2 min of irradiation.

type II mechanism ($^1O_2$) [28,33]. However, the mechanism of Iz formation from G in duplex DNA is not well understood. Thus, we analyzed the products of photoirradiated 5′-d(AAAAAAGGAAAAAA)/5′-d(TTTTTTCCTTTTTT) in the presence of riboflavin or AQ carboxylate. After various UV irradiation periods, photooxidized oligomers were digested with P1 nuclease and alkaline phosphatase at 4°C for 12 h and analyzed by HPLC. Under these prolonged low-temperature digestion conditions the undesired decomposition of dIz was reduced $<10\%$ as described in a previous report [30]. Typical HPLC profiles of enzymatic digestion of the reaction mixture and the results of the quantitative analysis are shown in Fig. 2. We found that the amount of 8-oxo-7,8-dihydro-2′-deoxyguanosine (8-oxodG) initially increased with decreasing dG, then decreased with dIz formation in both cases. The yield of dIz with respect to the degradation of dG was 5–10% which roughly corresponds to 50% of 8-oxodG.

2.2. Formation of Iz from 8-oxoG during photoirradiation of AQ-linked oligomer

To investigate whether or not Iz is formed from 8-oxoG through long-range hole migration, we photoirradiated an AQ-linked oligomer with a complementary oligomer containing 8-oxoG. In this system, the contribution of type II mechanism ($^1O_2$) is negligible. Fig. 3 shows the HPLC analysis of enzymatic digest of the AQ-linked oligomer before and after UV irradiation. The results showed that dIz formed from 8-oxodG under irradiation conditions.

2.3. Estimation of the strength of the Iz·G base pair

We estimated the stabilization energy of an Iz·G base pair by ab initio molecular orbital (MO) calculations using a SCRF method (ε of water) at a level of 6-31G*. In agreement with the preliminary MO calculation in vacuo [30], the stabilization energies of the Iz·G base pair were comparable or slightly less than that of a C·G base pair in water. The estimated distance between C1′–C1′ of the Iz·G base pair was 11.7 Å, which is slightly larger than that of the C·G base pair (10.6 Å). The electrostatic potential surface of Iz·G and C·G base pairs and stabilization energies shown in Fig. 4 indicate that the likelihood of Iz forming a base pair with G is very high.

2.4. Specific incorporation of G opposite Iz

To test the hypothesis of base pairing of Iz with G, we performed a primer extension assay to determine which nucleotides are incorporated into DNA opposite Iz. A 14-mer template containing Iz (Fig. 5a) was prepared by photooxidation of 5′-d(CCCAGTTCAAAATC) and purified by HPLC. The structure was characterized by enzymatic digestion and electro-spray mass spectrometry (ESI-MASS). Primer extension was performed by DNA polymerase I (pol I) having 5′ → 3′ exonuclease activity at 37°C for 10 min using 5′-Texas red-labeled 9-mer primers and the 14-mer template. The results of polyacrylamide gel electrophoresis are shown in Fig. 5b. HPLC analysis indicated that 98% of the template containing Iz remained under these conditions. Control experiments consisted of

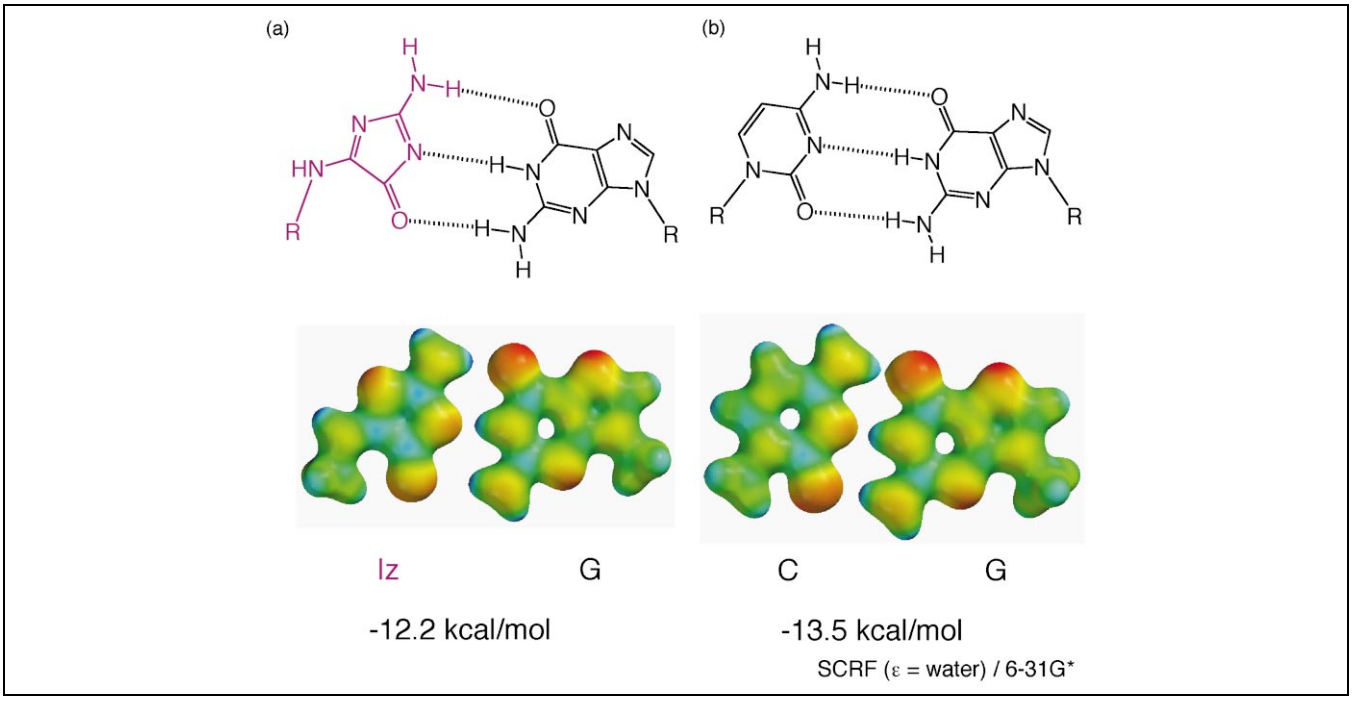

Fig. 4. Electrostatic populations and energies of (a) proposed Iz·G and (b) Watson–Crick C·G base pairs.

templates containing C (X = C) (lanes 1, 3, 5. 7 and 9) and containing Iz (X = Iz) (lanes 2, 4, 6, 8 and 10). We also compared the incorporation of adenine opposite 8-oxoG (lanes 12 and 14). Extension in the presence of a single dNTP (lanes 1–8) indicated that only G is incorporated opposite both Iz and C. Even in the presence of the Klenow fragment of pol I (Kf) lacking 5′→3′ exonuclease activity, G was incorporated opposite Iz (data not shown). Lanes 9 and 10 show that after G incorporation opposite Iz, pol I continued to extend 27% of the oligomer to its full length (14-mer), which roughly corresponds to that when A is opposite 8-oxoG (lanes 13 and 14).

2.5. Kinetic parameters of G insertion

We measured the kinetic parameters of G insertion. The Michaelis constant, K_m, the maximum rate of the reaction, V_{max} were determined using pol I and Kf (Table 1). The frequency of incorporation of G opposite Iz was 4.2% compared with that incorporated opposite C, and this frequency was comparable to that of A incorporation opposite 8-oxoG [10]. However, the chain extension of T from an Iz·G pair was only 6% of that of an 8-oxoG·A pair.

2.6. DNA polymerization using dIzTP

To confirm the formation of specific Iz·G pairs, we polymerized DNA using dIzTP, a 50-mer template and 5′-Texas red-labeled 20-mer primers (Fig. 6a). dIzTP was prepared from dGTP by photosensitization with riboflavin, purified by HPLC and structurally characterized by ESI-MASS and enzymatic dephosphorylation. The products of the primer extension reaction using Kf resolved by polyacrylamide gel electrophoresis are shown in Fig. 6b. In the absence of dIzTP, polymerization stopped at the T immediately before the first C, and G was not incorpo-

Table 1
Steady-state kinetic parameters for dGTP or dATP insertion opposite X in templates using pol I and for dTTP chain extension using Kf

System	V_{max} (%/min)	[pol I] (mU/μl)	K_m (μM)	F_{ins} (%)
dGTP 9mer-↓ 9mer-CACCC	36.5	0.50	1.10	100
dGTP 9mer-↓ 9mer-IzACCC	16.2	11.1	0.52	4.2
dATP 9mer-↓ 9mer-TACCC	16.9	0.63	0.73	100
dATP 9mer-↓ 9mer-^{8O}GACCC	36.0	1.25	12.1	6.4

System	V_{max} (%/min)	[Kf] (mU/μl)	K_m (μM)	F_{ext} (%)
dTTP 9mer-G↓ 9mer-CACCC	45.2	0.25	3.27	100
dTTP 9mer-G↓ 9mer-IzACCC	24.9	2.5	16.3	1.1
dTTP 9mer-A↓ 9mer-TACCC	18.7	0.31	0.67	100
dTTP 9mer-A↓ 9mer-^{8O}GACCC	19.2	1.0	1.30	18

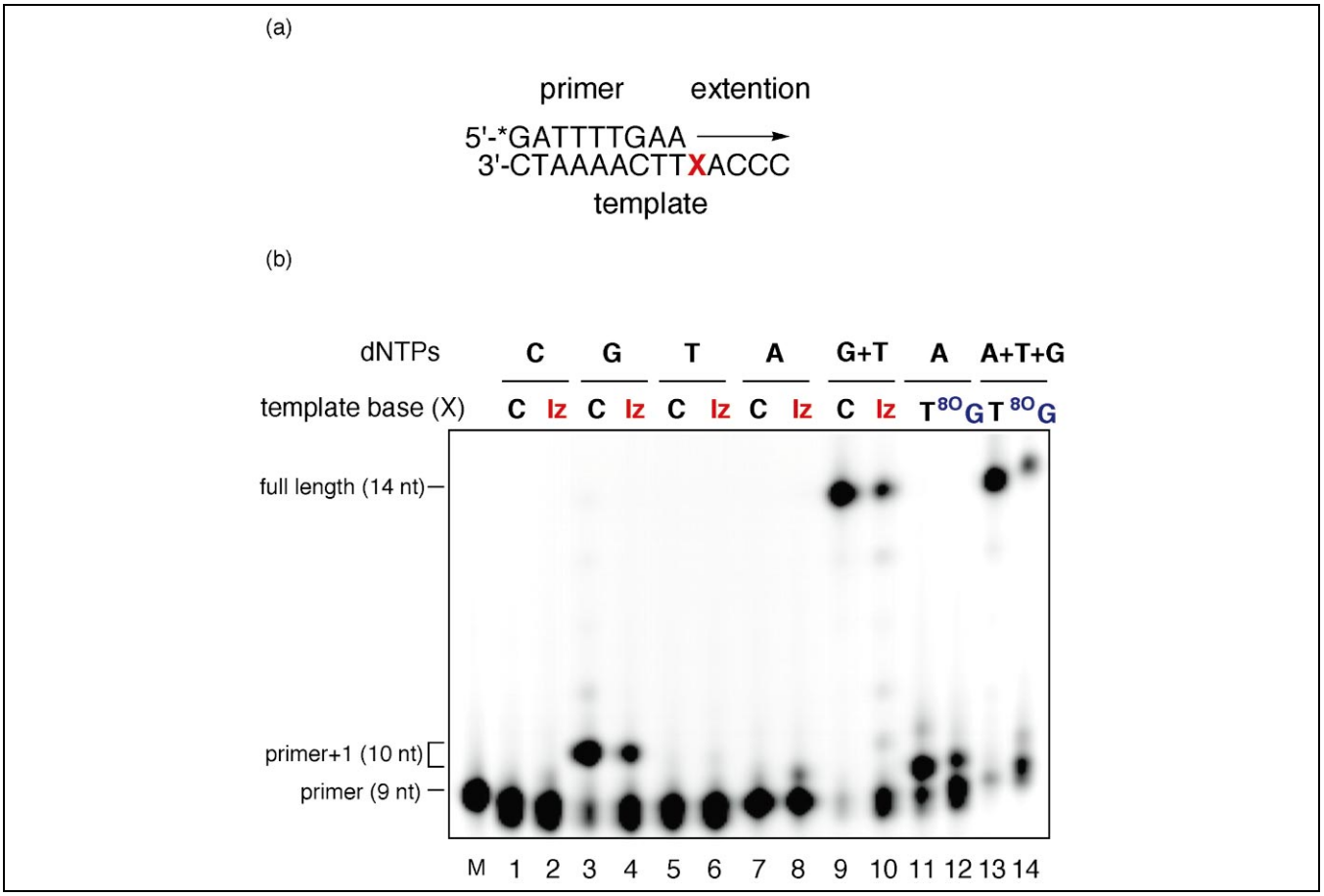

Fig. 5. Primer extension assay to identify nucleotides opposite Iz incorporated by pol I. (a) Sequences of template and primer were 5′-d(CCCAXTTCAAAATC)-3′ and 5′-Texas red-d(GATTTTGAA)-3′, respectively. (b) Concentration of triphosphate was 0.8 μM (final) and the amount of pol I was 0.5 U. Lanes 1, 3, 5, 7 and 9, template **1** (X = C); lanes 2, 4, 6, 8 and 10, template **2** (X = Iz); lanes 11 and 13, template **3** (X = T); lanes 12 and 14, template **4** (X = 8-oxoG). Lanes 1 and 2, dCTP; lanes 3 and 4, dGTP; lanes 5 and 6, dTTP; lanes 7 and 8, dATP; lanes 9 and 10, dGTP and dTTP; lanes 11 and 12, dATP; lanes 13 and 14, dGTP, dTTP and dATP.

rated opposite G under these conditions (lane 2). However, the primer was extended to produce fragments of nearly full length in the presence of dIzTP (lane 3). These fragments migrated slightly faster than those of the full length containing normal nucleotides (lane 1). These results indicated that dIzTP is incorporated opposite G in the same manner as dCTP. Moreover, in the presence of an appropriate ratio of dIzTP to dCTP (250:1), the control primer was fully extended (lane 4). Heating with piperidine (90°C, 20 min) degraded the faster migrating fragments into four new bands that appeared at all G sites (lane 5). These results are consistent with those of previous reports indicating that sites containing Iz are quantitatively cleaved by hot piperidine [30,32] and demonstrate that dIzTP was specifically incorporated opposite G. In contrast to dIzTP, 8-oxodGTP is incorporated opposite C and A with comparable frequency [7].

3. Discussion

Oxidative guanine damage in double helical DNA predominantly causes G·C→T·A and G·C→C·G transversion. Therefore, the biological impact of oxidation products of the G residue in DNA has been extensively investigated [10,34]. Since 8-oxoG is the most typical oxidation product of G, it can be used as a convenient marker of cellular oxidative stress. Because 8-oxo-G is chemically stable and can be electrochemically detected at high sensitivity [4,6–12]. DNA polymerase extension using a template containing 8-oxoG has demonstrated that dATP is incorporated opposite 8-oxoG [10]. In fact, structural studies have demonstrated that 8-oxoG can pair with A in the Hoogsteen mode and 8-oxoG·A base pairs are believed to cause G·C→T·A transversion mutations [9]. Since dGTP is not incorporated opposite 8-oxoG, 8-oxoG is not responsible for G·C→C·G transversion. The frequency of G·C→C·G transversions is considerably higher under oxidative stress [13–26], and G·C→C·G transversions are found in important genes. For example, the GGT→CGT mutation is frequent at codons 12 and 13 of the ras gene [35,36]. In contrast to G·C→T·A transversions, the oxidative lesion that causes G·C→C·G transversions is not known.

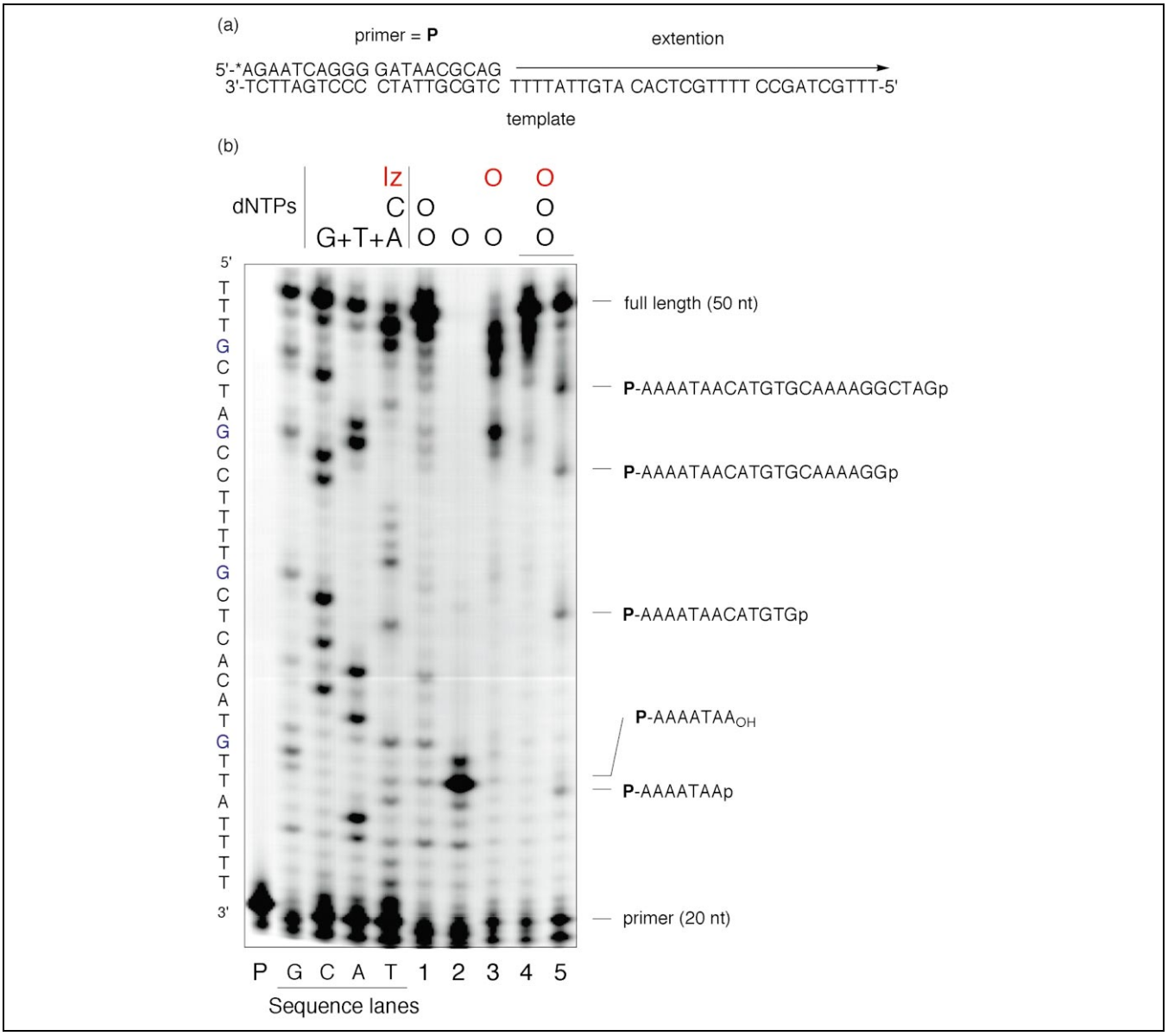

Fig. 6. Primer extension assay to incorporate dIzTP opposite G using Kf. (a) Sequence of template is 5′-d(TTTGCTAGCCTTTTGCTCACATGTTATTTTCTGCGTTATCCCCTGATTCT)-3′ and that of primer is 5′-Texas red-d(AGAATCAGGGGATAACGCAG)-3′. (b) Sequencing by the Sanger method. The amount of Kf was 0.5 U. Lanes: 1, four normal dNTP (0.88 μM each); 2, dGTP, dTTP and dATP (0.88 μM each); 3, dIzTP (27 μM), dGTP, dTTP and dATP (0.88 μM each); 4, dIzTP (27 μM), dCTP reaction (11 nM), dGTP, dTTP and dATP (0.88 μM each); 5, reaction mixture of lane 4 heated with piperidine (1 M, 90°C, 20 min).

Cadet et al. identified thermally unstable dIz ($t_{1/2}$ = 147 min at 37°C) and dOz as oxidation products of dG [28,29]. The same group demonstrated that Oz induces dATP insertion during DNA synthesis, suggesting that Oz can cause G·C→T·A transversions [34]. In addition to Oz they also demonstrated that oxaluric acid and cynuric acid can also cause G·C→T·A transversions [37,38]. Independently, we demonstrated that oxidative DNA damage is localized at the 5′-GG-3′ site [39] and that Iz is formed at 5′-GG-3′ sites in double helical DNA [30]. Based on this observation we proposed the notion that Iz forms base pairs with G to induce G·C→C·G transversions. In fact, MO calculation suggests that the Iz·G base pair possesses comparable or slightly less stability relative to that of a Watson–Crick C·G base pair in water. The electrostatic potential surface of Iz shows donor and acceptor abilities of H bonding closely resemble to C.

To understand the mechanism of Iz formation, we investigated the photooxidation of various oligonucleotides in the presence of riboflavin or AQ. In agreement with other observations, the amount of Iz formed was significant in duplex DNA. However, product analysis after various irradiation periods demonstrated that Iz formed by the further oxidation of 8-oxoG. Burrows et al. have re-

ported that dGTP is incorporated opposite a further oxidized product of 8-oxoG which is not Iz according to TOF MASS and the structure of this product has not been elucidated [27].

Long-range guanine oxidation through a DNA base π-stack has been observed using a range of tethered oxidants [40–44] and 8-oxoG is a major oxidation product of this system [43]. Since the redox potential of 8-oxoG is significantly lower than that of G [45], forming 8-oxoG would be a better oxidative target than G in duplex DNA [27,44]. To examine whether forming 8-oxoG is oxidized through long-range hole migration, we photoirradiated a covalently AQ-linked oligomer with a complementary oligomer containing 8-oxoG. Analysis by HPLC indicated that 8-oxodG is consumed, yielding dIz as the UV (254 nm) detectable product. The present results clearly demonstrated that Iz is produced from 8-oxoG through long-range hole migration and suggest the possible role of Iz in long-range oxidative DNA damage.

To test the hypothesis of Iz·G base pair formation, we performed two sets of DNA polymerizations. We initially polymerized DNA using a template containing Iz. The results shown in Fig. 5 demonstrate that only G was specifically incorporated opposite Iz during primer extension in vitro, suggesting that Iz·G base pairs play a role in G·C → C·G transversion mutations. The incorporation of G opposite Iz was very specific and there was no bypass for Iz template. This finding suggests that once Iz is formed in template DNA, replication slows down to wait for dGTP, thus increasing the frequency of G·C → C·G transversions. This is in clear contrast to the fact that considerable non-mutagenic C is incorporated opposite 8-oxoG in addition to mutagenic incorporation of A. Kinetic analysis indicated that the frequency of G incorporation opposite Iz was comparable to that of A incorporation opposite 8-oxoG. These results suggest that Iz·G is responsible for G·C → C·G transversions. However, the amount of chain extension of T from an Iz·G pair was only 6% of that of an 8-oxoG·A pair. The low efficiency of extension from Iz·G pairs is probably due to insufficient stacking interaction between Iz and T base of dTTP relative to that of 8-oxoG and T, since the importance of base stacking between the primer terminal and incorporated nucleoside triphosphate are demonstrated in the replication complex [46]. Presumably due to chemical instability, the biological impact of Iz might be underestimated. However, Ikeda and Saito recently reported that Iz is stabilized in a double helical DNA structure and that the half-life of Iz under this condition is about 20 h at 37°C which is significantly longer than that of dIz (monomer) [47]. Therefore, DNA replication before hydrolysis to Oz may cause G·C → C·G transversions.

We then performed the 'reverse' experiment of the first DNA polymerization using dIzTP and a natural DNA template. Primer extension demonstrated that dIzTP is specifically incorporated opposite every G site. These findings are in direct contrast to the ambiguous incorporation of 8-oxodGTP into A and C templates [7] and further support the notion of specific Iz·G base pair formation. The biological role of Iz in mutagenesis and its repair mechanisms should be addressed at the molecular and cellular levels.

4. Significance

Although the frequency of G·C → C·G transversions is quite high under oxidative stress, the oxidative lesion that causes G·C → C·G transversions is unknown. Primer extension indicated that only dGTP is specifically incorporated opposite Iz. DNA polymerization using a natural DNA template demonstrated that dIzTP is incorporated opposite G. These results suggest the specific formation Iz·G base pairs in vitro. Iz·G base pairs may cause G·C → C·G transversion mutations.

5. Materials and methods

5.1. Calculations of base pairs

The base pairs were calculated using Gaussian 94 and Spartan (version 5.0) programs on a Silicon Graphics O_2 R10000. The geometry of the base pairs and the isolated bases were constructed using the builder module in the Spartan program. All the sugar backbones of complementary bases were removed except for the 2′-deoxyribose C1′ carbon and C1′ H. Two H atoms were then attached to the C1′ methine to complete the *N*-methylated nucleobases. The geometry was optimized at the 6-31G* level, and single point energy was corrected at the same level for the zero-point vibrational energy (ZPE), the basis set superposition error (BSSE) and the reorganization energy [48,49]. The calculated heat of formation of base pairs was defined as: $\Delta E = E$(base pair complex 'X·Y')−[E(isolated base 'X')+E(isolated base 'Y')]. To estimate energy in water ($\varepsilon = 78.54$), we calculated the self-consistent reaction field (SCRF) value using the Onsager reaction field model.

5.2. Photoirradiation of oligonucleotides

A mixture containing oligomer (71.4 μM strand concentration) with free or ODN-linked sensitizer in 50 mM sodium cacodylate buffer (pH 7.0) was irradiated at 365 nm under aerobic conditions at 0°C for the indicated periods from a distance of 5 cm. Thereafter, the samples were digested with alkaline phosphatase (23 units/ml) and P1 nuclease (14 units/ml) at 4°C for 12 h [30]. Low-temperature enzymatic digestion of these samples was analyzed by HPLC using a 5C18-MS column (5 μm, 150×4.6 mm, elution with a solvent mixture of 50 mM ammonium formate, 0% (isocratic) acetonitrile/0–5 min, 0–7%/5–27 min and 7% (isocratic)/27–30 min at a flow rate of 1.0 ml/min) and monitored at 254 nm.

5.3. Synthesis of AQ-linked oligonucleotide

The phosphoramidite of *N*-(2-hydroxy-ethyl)-2-anthraquinone carboxamine (AQ) was synthesized from anthraquinone-2-carboxylic acid [41] and AQ-linked oligonucleotide was synthesized on a Beckman DNA synthesizer. The concentration of these oligonucleotides was determined by enzymatic digestion. These oligonucleotides were identified by ESI-MASS (negative mode). ESI-MASS, AQ-linked 5′-d(TTTTTTCTTTTTT): 4234.1 (4234.8, calculated). Enzymatic digestion of AQ-linked 5′-d(TTTTTTCTTTTTT), provided AQ-dT, which was eluted at 8 min after dA on a 5C18-MS column (5 μm, 150×4.6 mm using a solvent mixture of 50 mM ammonium formate, 0–30% acetonitrile/0–20 min and 30%(isocratic)/20–22 min at a flow rate of 1.0 ml/min). AQ-dT was identified by ESI-MASS (negative mode). ESI-MASS, AQ-dT: 599.3 (599.5, calculated).

5.4. Synthesis of imidazolone containing oligonucleotides

A solution of 5′-d(CCCAGTTCAAAATC)-3′ (18.7 μM) and riboflavin (50 μM) in sodium cacodylate buffer (50 mM, pH 7.0) was irradiated with UV at 0°C for 20 min (365 nm). The corresponding oligonucleotide 5′-d(CCCAIzTTCAAAATC)-3′ containing imidazolone (Iz) (**2**) was purified by passage through a 5C18-MS column (5 μm, 150×4.6 mm) using a gradient of acetonitrile (5–7%/0–30 min and 7% (isocratic)/30–40 min) in 50 mM ammonium formate at a flow rate of 1.0 ml/min). Oligonucleotides were detected at 254 nm using a UV–visible spectrophotometer and the yield of **2** was 38% of the consumed 14-mer, 5′-d(CCCAGTTCAAAATC)-3′ (**1**). Fractions containing Iz were collected and acetonitrile was evaporated under reduced pressure. The sample was loaded on the same column and desalted with water at a flow rate of 1.0 ml/min, then eluted with 50% aqueous acetonitrile. The acetonitrile was evaporated under reduced pressure, and the sample was lyophilized. The concentration of **2** was determined by comparison with that of **1**. The purity was >92% as judged by HPLC. The structure of **2** was elucidated by enzymatic digestion as described above and by ESI-MASS. Enzymatic digestion of **2** provided dC:dIz:dT:dA = 5:1:3:5. ESI-MASS, **2**: 4152.0 (4152.8, calculated).

5.5. Polymerase reaction

Reactions catalyzed by pol I or Kf (Boehringer Mannheim) proceeded in 50 μl of 10 mM Tris–HCl (pH 7.4), 5 mM $MgCl_2$, 7.5 mM DTT and 2.5 μg BSA containing 1.5 pmol of the template and 1.0 pmol of primer 5′ end-labeled with Texas red. The constituents were mixed at room temperature, then cooled to 0°C for >5 min. The DNA was polymerized using dNTP and polymerase at 37°C for 10 min. Details of the conditions are shown in the legends to Fig. 5. Reactions were stopped by adding 2 μl of 0.5 mM sodium EDTA. The samples (50 μl) were dried or ethanol-precipitated, then dissolved in 10 μl of loading dye (formamide with fuchsin red). An aliquot (2 μl) was resolved by electrophoresis on 20% polyacrylamide gels and sequenced (5500S DNA sequencer, Hitachi). Fluorescent bands were analyzed using FRAGLYS2 (version 2.2, Hitachi) and NIH image (version 1.61) on a Power Macintosh G3.

5.6. Steady-state kinetics

Steady-state kinetic parameters were established for dGTP insertion opposite X (**1**: X = C, **2**: X = Iz) in templates using pol I and for dTTP chain extension from X:G pairs from the 3′ primer terminus using Kf. Enzyme and nucleoside triphosphate concentrations were adjusted for insertion or chain extension reactions to allow 1–20% yields. The temperature of the 1 min reactions was 25°C. The Michaelis constant (K_m) and maximum rate of reaction (V_{max}) were obtained from Lineweaver–Burk plots of the kinetic data (the average of two separate experiments). Frequencies of insertion (F_{ins}) and extension (F_{ext}) were determined relative to C·G base pairs according to the equation $F = (V_{max}/K_m\ [\text{polymerase}])_{(Iz\cdot G)}/(V_{max}/K_m\ [\text{polymerase}])_{(C\cdot G)}$. Steady-state kinetic parameters were checked for dATP insertion opposite X (**3**: X = T, **4**: X = 8-oxoG) in templates and for dTTP chain extension from X·A pairs originating at the 3′ primer terminus as controls. The F_{ins} and F_{ext} values of 8-oxoG were determined relative to the T·A base pairs according to the equation $F = (V_{max}/K_m\ [\text{polymerase}])_{(8-oxoG\cdot A)}/(V_{max}/K_m\ [\text{polymerase}])_{(T\cdot A)}$.

5.7. Preparation of dIzTP

A solution containing dGTP (50 μM) and riboflavin (94.5 μM) in sodium cacodylate buffer (50 mM, pH 7.0) was irradiated with UV at 0°C for 20 min (365 nm). Deoxy-IzTP was purified on a 5C18-ARII column (5 μm, 150×4.6 mm) using a gradient of acetonitrile (2–4%/0–20 min) in 100 mM triethylammonium bicarbonate at a flow rate of 0.9 ml/min). The oligonucleotides were detected at 254 nm using a UV–visible spectrophotometer. The structure of dIzTP was elucidated by enzymatic digestion (calf intestine alkaline phosphatase) and by ESI-MASS dIzTP: 467.9 (468.1, calculated). The yield of dIzTP from dGTP was 31%.

Acknowledgements

This study was partly supported by a Grant-in-Aid for Priority Research from the Ministry of Education, Science, Sports, and Culture, Japan, The Sagawa Foundation for Promotion of Cancer Research, and from the Atsuko Ohuchi Memorial Fund (Tokyo Medical and Dental University). K.K. is a research fellow of the Japan Society for the Promotion of Science.

References

[1] E.C. Friedberg, G.C. Walker, W. Siede, DNA Repair and Mutagenesis, ASM, Washington, DC, 1995.
[2] B.N. Ames, M.K. Shigenega, T.M. Hagen, Oxidants, antioxidants and the degenerative diseases of aging, Proc. Natl. Acad. Sci. USA 90 (1993) 7915–7922.

[3] T. Lindahl, R.D. Wood, Quality control by DNA repair, Science 286 (1999) 1897–1905.
[4] R. Lu, H.M. Nash, G.L. Verdine, A mammalian DNA repair enzyme that excises oxidatively damaged guanines maps to a locus frequently lost in lung cancer, Curr. Biol. 7 (1997) 397–407.
[5] S. Steenken, S.V. Jovanovic, How easily oxidizable is DNA? One-electron reduction potentials of adenosine and guanosine radicals in aqueous solution, J. Am. Chem. Soc. 119 (1997) 617–618.
[6] H. Kasai, S. Nishimura, in: H. Sies (Ed.), Oxidative Stress II: Oxidants and Antioxidants, Academic Press, New York, 1991, pp. 99–116.
[7] H. Maki, M. Sekiguchi, MutT protein specifically hydrolyses a potent mutagenic substrate for DNA synthesis, Nature 355 (1992) 273–275.
[8] S.D. Brunner, D.P.G. Norman, G.L. Verdine, Structural basis for recognition and repair of the endogenous mutagen 8-oxoguanine in DNA, Nature 403 (2000) 859–866.
[9] A.P. Grollman, M. Moriya, Mutagenesis by 8-oxoguanine: An enemy within, Trends Genet. 9 (1993) 246–249.
[10] S. Shibutani, M. Takeshita, A.P. Grollman, Insertion of specific bases during DNA systhesis past the oxidation-damaged base 8-oxodG, Nature 349 (1991) 431–434.
[11] L.A. Lipscomb, M.E. Peek, M.L. Morningstar, S.M. Verghis, E.M. Miller, A. Rich, J.M. Essigmann, L.D. Williams, X-ray structure of a DNA decamer containing 7,8-dihydro-8-oxoguanine, Proc. Natl. Acad. Sci. USA 92 (1995) 719–723.
[12] M. Moriya, Single-stranded shuttle phagemid for mutagenesis studies in mammalian cells: 8-Oxoguanine in DNA induces targeted G:C → T:A transversions in simian kidney cells, Proc. Natl. Acad. Sci. USA 90 (1993) 1122–1126.
[13] T.J. Mcbride, J.E. Schneider, R.A. Floyd, L.A. Loeb, Mutations induced by methylene blue plus light in single-stranded M13mp2, Proc. Natl. Acad. Sci. USA 89 (1992) 6866–6870.
[14] T. Ono, K. Negishi, H. Hayatsu, Spectra of superoxide-induced mutations in the *lacI* gene of a wild-type and a *mutM* strain of *Escherichia coli* K-12, Mutat. Res. 326 (1995) 175–183.
[15] T.J. Mcbride, B.D. Preston, L.A. Loeb, Mutagenic spectrum resulting from DNA damage by oxygen radicals, Biochemistry 30 (1991) 207–213.
[16] A.R. Oller, W.G. Thilly, Mutational spectra in human B-cells: Spontaneous, oxygen and hydrogen peroxide-induced mutations at the *hprt* gene, J. Mol. Biol. 228 (1992) 813–826.
[17] K. Takimoto, K. Tano, M. Hashimoto, M. Hori, S. Akasaka, H. Utsumi, Delayed transfection of DNA after riboflavin mediated photosensitization increases G:C to C:G transversions of *supF* gene in *Escherichia coli mutY* strain, Mutat. Res. 445 (1999) 93–98.
[18] F. Maehira, I. Miyagi, T. Asato, Y. Eguchi, H. Takei, K. Nakatsuki, M. Fukuoka, F. Zaha, Alterations of protein kinase C, 8-hydroxydeoxyguanosine, and K-ras oncogene in rat lungs exposed to passive smoking, Clin. Chim. Acta 289 (1999) 133–144.
[19] K. Negishi, W. Hao, Spectrum of mutations in single-stranded DNA phage M13mp2 exposed to sunlight: predominance of G-to-C transversion, Carcinogenesis 13 (1992) 1615–1618.
[20] N.J. Sargentini, K.C. Smith, DNA sequence analysis of γ-radiation (anionic)- induced and spontaneous *lacI* mutations in *Escherichia coli* K-12, Mutat. Res. 309 (1994) 147–163.
[21] S. Akasaka, K. Yamamoto, Hydrogen peroxide induces G:C to T:A and G:C to C:G transversions in the *supF* gene of *Escherichia coli*, Mol. Gen. Genet. 243 (1994) 500–505.
[22] M.R. Valentine, H. Rodriguez, J. Termini, Mutagenesis by peroxy radical is dominated by transversions at deoxyguanosine: evidence for the lack of involvement of 8-oxo-dG and/or abasic site formation, Biochemistry 37 (1998) 7030–7038.
[23] S. Emmert, B. Epe, C.R. Saha-Möller, W. Adam, T.M. Rünger, Assessment of genotoxicity and mutagenicity of 1,2-dioxetanes in human cells using a plasmid shuttle vector, Photochem. Photobiol. 61 (1995) 136–141.
[24] H. Shimamura, S. Akasaka, K. Kubo, Y. Saito, S. Nakajima, K. Tano, H. Utsumi, K. Yamamoto, Mutational specificity of the ferrous ion in a *supF* gene of endonuclease III/VIII deficient *Escherichia coli*, J. Radiat. Res. 38 (1997) 165–171.
[25] K. Tano, S. Akasaka, M. Hashimoto, M. Asano, K. Yamamoto, H. Utsumi, K. Takimoto, Specificity of mutations induced by riboflavin mediated photosensitization in the *supF* gene of *Escherichia coli*, Mutat. Res. 420 (1998) 7–13.
[26] I. Schulz, H.-C. Mahler, S. Boiteux, B. Epe, Oxidative DNA base damage induced by singlet oxygen and photosensitization: recognition by repair endonucleases and mutagenicity, Mutat. Res. 461 (2000) 145–156.
[27] V. Duarte, J.G. Muller, C.J. Burrows, Insertion of dGMP and dAMP during in vitro DNA synthesis opposite an oxidized form of 7,8-dihydro-8-oxoguanine, Nucleic Acids Res. 27 (1999) 496–502.
[28] J. Cadet, M. Berger, G.W. Buchko, P.C. Joshi, S. Raoul, J.-L. Ravanat, 2,2-Diamino-4-[(3,5-di-*O*-acetyl-2-deoxy-β-D-*erythro*-pentofuranosyl)amino]-5-(2*H*)-oxazolone: a novel and predominant radical oxidation product of 3′, 5′-di-*O*-acetyl-2′-deoxyguanosine, J. Am. Chem. Soc. 116 (1994) 7403–7404.
[29] S. Raoul, M. Berger, G.W. Buchko, P.C. Joshi, B. Morin, M. Weinfeld, J. Cadet, ^{1}H, ^{13}C and ^{15}N Nuclear magnetic resonance analysis and chemical features of the two main radical oxidation products of 2′-deoxyguanosine: oxazolone and imidazolone nucleosides, J. Chem. Soc. Perkin Trans. 2 (1996) 371–381.
[30] K. Kino, I. Saito, H. Sugiyama, Product analysis of GG-specific photooxidation of DNA via electron transfer: 2-aminoimidazolone as a major guanine oxidation product, J. Am. Chem. Soc. 120 (1998) 7373–7374.
[31] C. Vialas, G. Pratviel, C. Claparols, B. Meunier, Efficient oxidation of 2′-deoxyguanosine by Mn-TMPyP/$KHSO_5$ to imidazole dIz without formation of 8-oxo-dG, J. Am. Chem. Soc. 120 (1998) 11548–11553.
[32] G.W. Buchko, J. Cadet, B. Morin, M. Weinfeld, Photooxidation of d(TpG) by riboflavin and methylene blue. Isolation and characterization of thymidylyl-(3′, 5′)-2-amino-5-[(2-deoxy-β-D-*erythro*-pentofuranosyl)amino]-*4H*-imidazol-4-one and its primary decomposition product thymidylyl-(3′,5′)-2, 2-diamino-4-[(2-deoxy-β-D-*erythro*-pentofuranosyl)amino]-5(2*H*)-oxazolone, Nucleic Acid Res. 23 (1995) 3954–3961.
[33] J. Cadet, C. Decarroz, S.Y. Wang, W.R. Midden, Mechanism and products of photosensitized degradation of nucleic acids and related model compounds, Isr. J. Chem. 23 (1983) 420–429.
[34] V. Duarte, D. Gasparutto, M. Jaquinod, J. Cadet, In vitro DNA synthesis opposite oxazolone and repair of this DNA damage using modified oligonucleotides, Nucleic Acids Res. 28 (2000) 1555–1563.
[35] W. Giaretti, A. Rapallo, E. Geido, A. Sciutto, F. Merlo, M. Risio, F.P. Rossini, Specific K-ras2 mutations in human sporadic colorectal adenomas are associated with DNA near-diploid aneuploidy and inhibition of proliferation, Am. J. Pathol. 153 (1998) 1201–1209.
[36] P. Moerkerk, J.W. Arend, M. van Driel, A. de Bruïne, A. de Goeij, J. ten Kate, Type and number of Ki-*ras* point mutations relate to stage of human colorectal cancer, Cancer Res. 54 (1994) 3376–3378.
[37] D. Gasparutto, S.D. Cruz, A.-G. Bourdat, M. Jaquinod, J. Cadet, Synthesis and biochemical properties of cyanuric acid nucleoside-containing DNA oligomers, Chem. Res. Toxicol. 12 (1999) 630–638.
[38] V. Duarte, D. Gasparutto, M. Jaquinod, J.-L. Ravanat, J. Cadet, Repair and mutagenic potential of oxaluric acid, a major product of singlet oxygen-mediated oxidation of 8-oxo-7, 8-dihydroguanine, Chem. Res. Toxicol. 14 (2001) 46–53.
[39] H. Sugiyama, I. Saito, Theoretical studies of GG-specific photocleavage of DNA via electron transfer: significant lowering of ionization potential and 5′-localization of HOMO of stacked GG bases in B-form DNA, J. Am. Chem. Soc. 118 (1996) 7063–7068.
[40] D.B. Hall, R.E. Holmlin, J.K. Barton, Oxidative DNA damage through long-range electron transfer, Nature 382 (1996) 731–735.
[41] S.M. Gasper, G.B. Schuster, Intramolecular photoinduced electron transfer to anthraquinones linked to duplex DNA: The effect of gaps

and traps on long-range radical cation migration, J. Am. Chem. Soc. 119 (1997) 12762–12771.

[42] E. Meggers, M.E. Michel-Beyerle, B. Giese, Sequence dependent long range hole transport in DNA, J. Am. Chem. Soc. 120 (1998) 12950–12955.

[43] M.R. Arkin, E.D.A. Stemp, S.C. Pulver, J.K. Barton, Long-range oxidation of guanine by Ru(III) in duplex DNA, Chem. Biol. 4 (1997) 389–400.

[44] E. Meggers, A. Dussy, T. Schäfer, B. Giese, Electron transfer in DNA from guanine and 8-oxoguanine to a radical cation of the carbohydrate backbone, Chem. Eur. J. 6 (2000) 485–492.

[45] F. Prat, K.N. Houk, C.S. Foote, Effect of guanine stacking on the oxidation of 8-oxoguanine in B-DNA, J. Am. Chem. Soc. 120 (1998) 845–846.

[46] S. Doublié, S. Tabor, A.M. Long, C.C. Richardson, T. Ellenberger, Crystal structure of a bacteriophage T7 DNA replication complex at 2.2 Å resolution, Nature 391 (1998) 251–258.

[47] H. Ikeda, I. Saito, 8-Methoxydeoxyguanine as an effective precursor of 2-aminoimidazolone, a major guanine oxidation product in one-electron oxidation of DNA, J. Am. Chem. Soc. 121 (1999) 10836–10837.

[48] C. Roberts, R. Bandaru, C. Switzer, Theoretical and experimental study of isoguanine and isocytosine: Base pairing in an expanded genetic system, J. Am. Chem. Soc. 119 (1997) 4640–4649.

[49] J. Florián, J. Leszczynski, Spontaneous DNA mutations induced by proton transfer in the guanine–cytosine base pairs: An energetic perspective, J. Am. Chem. Soc. 118 (1996) 3010–3017.